Surface & Coatings Technology 206 (2011) 1484–1489

Contents lists available at SciVerse ScienceDirect

Surface & Coatings Technology

journal homepage: www.elsevier.com/locate/surfcoat

An XPS and ellipsometry study of Cr–O–Al mixed oxides grown by reactive magnetron sputtering

N. Benito [a], D. Díaz [a], L. Vergara [b], R. Escobar Galindo [b], O. Sánchez [b], C. Palacio [a,*]

[a] Departamento de Física Aplicada, Facultad de Ciencias, Módulo 12. Universidad Autónoma de Madrid, Cantoblanco, 28049, Madrid, Spain
[b] Instituto de Ciencia de Materiales de Madrid, Consejo Superior de Investigaciones Científicas, Cantoblanco, 28049, Madrid, Spain

ARTICLE INFO

Article history:
Received 29 June 2011
Accepted in revised form 13 September 2011
Available online 19 September 2011

Keywords:
Cr–O–Al mixed oxides
Reactive sputtering
ARXPS
Preferential sputtering

ABSTRACT

Cr–O–Al thin film mixed oxides grown on Si (100) substrates by reactive magnetron sputtering using different target compositions from 90% Cr (10% Al) to 10% Cr (90% Al) and oxygen fluxes in the range from 0 to 15 sccm have been investigated using ex situ XPS, XPS depth profiles and ARXPS. The chemical information obtained with XPS as well as the observed chemical shift of the Cr 2p, Al 2s and O 1s bands points to the formation of mixed substitutional Me_2O_3 oxides (Me = Al + Cr) instead of the formation of single oxide phases. Compositions and stoichiometries obtained from concentration depth profile measurements (CDP) simultaneously using XPS and Ar^+ bombardment confirm the formation of such a type of substitutional mixed oxides. ARXPS allows ruling out oxygen preferential sputtering during Ar^+ bombardment. Finally, it is shown that the optical properties of the films like their refractive index can be controlled through their chemical composition.

1. Introduction

The enormous development of thin film deposition and characterization techniques has led to a big progress in different scientific and technological areas like corrosion, catalysis, electronics, optical applications, etc. [1–7]. Nowadays, the synthesis and characterization of mixed oxide thin films is a field of interest because the properties of the formed compound can be improved with respect to those of the individual oxides and adapted to specific requirements by modifying the thickness, structure, porosity, morphology and composition of the film [6]. It is expected that not only the refractive index, but also other properties of the mixed oxide, like its band gap or its electrical permittivity, be somewhere in between those of the pure oxides in such a way that materials with properties not available for pure oxides can be obtained. Since chromium oxide (Cr_2O_3) is the hardest oxide that also exhibits low friction coefficient, high wear and corrosion resistance, chemical inertness and good optical characteristics [8–10], Cr–O–Si and Cr–O–Al are, among the different mixed oxides, very good candidates to be used for tribological applications (protective coatings), optical applications (solar absorber materials), microelectronic applications, etc. [11,12]. In a recent publication, we have presented experimental results on the growth of thin film Cr–O–Si mixed oxides by reactive magnetron sputtering to be used as optical coatings in which we have been able to vary the refractive index of the mixed oxides in a controlled way between those of each of their constituent single oxides [13]. Therefore, as a continuation of this previous publication, the purpose of this work is to explore the synthesis of Cr–O–Al mixed oxides by reactive magnetron sputtering using X-ray photoelectron spectroscopy (XPS) and angle resolved X-ray photoelectron spectroscopy (ARXPS) as analytical tools. The BE shift of the XPS bands associated with Cr, Al and O has been used along with ellipsometry measurements to conclude the formation of ternary compounds instead of single oxide phases. In order to obtain chemical information, the concentration depth profiles (CDP) of the formed films have been obtained using XPS and simultaneous Ar^+ bombardment at low energy (3 keV). ARXPS has been used to rule out any preferential erosion during CDP measurements. The influence of the target stoichiometry and of the oxygen flux on the film composition has also been studied.

2. Experimental

Mixed aluminium and chromium oxide films were deposited on (100) silicon substrates by DC magnetron sputtering of chromium/aluminium compound targets with relative percentage atomic ratios of Cr/Al = 90/10, 75/25, 25/75 and 10/90 in a high-purity (99.999%) argon and oxygen atmosphere. The sputtering chamber was pumped down to a base pressure below 8.6×10^{-4} Pa before letting in the gas mixture. The flux of argon was kept fixed at 80 sccm while the amount of oxygen in the reactive gas was varied (between 1.25 and 12.5 sccm) for a working pressure of around 1 Pa and 100 W of DC power. Prior to the deposition of each sample, while covering the substrates with a shutter, the target was sputtered with argon for 10 min in order to clean its surface, and then oxygen was let inside the chamber. Only after the target was oxidized (i. e. "poisoned") was the

* Corresponding author.
E-mail address: carlos.palacio@uam.es (C. Palacio).

0257-8972/$ – see front matter © 2011 Elsevier B.V. All rights reserved.
doi:10.1016/j.surfcoat.2011.09.026

Table 1
Experimental parameters used for the growth of the different coating studied.

Sample	Cr_{target} (at.%)	Al_{target} (at.%)	O_2 flux (sccm)	Thickness (nm)
CrAl9010	90	10	1.25	532 ± 16
			5	36 ± 2
			12.5	33 ± 2
CrAl7525	75	25	1.25	550 ± 17
CrAl2575	25	75	1.25	370 ± 11
CrAl1090	10	90	1.25	356 ± 10
			5	15 ± 3
			12.5	25 ± 2

shutter removed. The substrate holder, placed at a distance of 12 cm from the target, was electrically isolated, with no bias voltage applied externally. Likewise, no intentional heating of the substrates was performed during deposition. The sputtering time was always kept fixed at 30 min, leading to different film thicknesses depending on the oxygen flux (see Table 1) that were determined with a Veeco Dektak 150 stylus surface profiler by measuring the height of a step left by a mechanical mask. Spectroscopic ellipsometry was employed to determine the refractive index and the absorption coefficient of the films in the visible range (from 400 nm to 900 nm); measurements were performed with an M-2000U ellipsometer working in the range of 250–1000 nm with an incidence angle of 70°.

XPS spectra were measured in an ultrahigh vacuum system at a base pressure below 8×10^{-8} Pa using a hemispherical analyzer (SPECS Phoibos 100 MCD-5). The pass energy was 9 eV giving a constant resolution of 0.9 eV. The Au $4f_{7/2}$, Ag $3d_{5/2}$ and Cu $2p_{3/2}$ lines of reference samples at 84.0, 368.3 and 932.7 eV, respectively, were used to calibrate binding energies. A twin anode (Mg and Al) X-ray source was operated at a constant power of 300 W using Mg Kα radiation for the XPS measurements. For depth profiling, ion bombardment was carried out at normal incidence using a penning ion source (SPECS IQP 10/63) with an ion beam energy of 3 keV, raising the pressure to 4×10^{-2} Pa of Ar^+. The ion beam current density, measured with a Faraday cup that can be placed in the same position as the sample holder, was 4.6 μA/cm^2. Those experimental conditions lead to an ion-beam with a flat profile greater than ~10 × 10 mm^2. For ARXPS measurements, the sample was placed in a sample stage with four degrees of freedom in such a way that the emission angle can be varied between 0º and 60º in order to perform angle resolved measurements.

3. Results and discussion

As pointed out in the experimental section, four sets of samples have been prepared using Cr/Al targets of nominal compositions 90/10, 75/25, 25/75 and 10/90 at.% and different oxygen flux. These samples will be denoted as CrAl9010, CrAl7510, CrAl2575 and CrAl1090, respectively (see Table 1). XPS analysis of all the films reveals a thin layer of C contamination. C 1s binding energy is at 285 eV for samples without any charging effects; however, with increasing Al contents, charging effects appear during XPS measurements due to the insulating character of these materials and then the measured C 1s binding energy (BE) has been used to correct such effect [14]. The contamination layer was removed by bombarding all samples with 3 keV Ar^+ ions at normal incidence. It is important to indicate that this cleaning procedure does not change the surface stoichiometry since, as we will discuss later, Cr_2O_3 and Al_2O_3 do not display preferential erosion effects during Ar^+ bombardment.

Fig. 1 shows (a) the Al 2p + Cr 3s, (b) the Al 2s, (c) the O1s and (d) the Cr 2p core level spectra of the Cr–O–Al mixed oxides obtained for the different target compositions and grown with an oxygen flux of 1.25 sccm. Instead of using reference spectra for comparative purposes, the binding energies of the respective core level spectra for pure Cr_2O_3 and Al_2O_3 compounds have been indicated by arrows. As

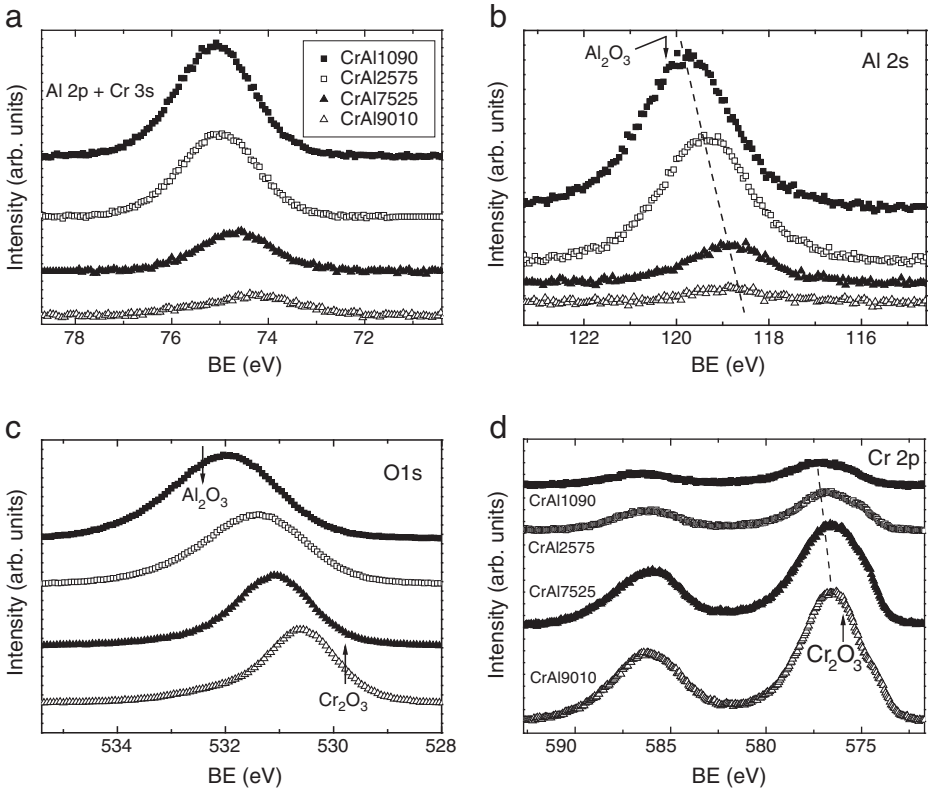

Fig. 1. (a) Al 2p + Cr 3s, (b) Al 2s, (c) O 1s and (d) Cr 2p core level spectra of the Cr–O–Al mixed oxides obtained for the different target nominal compositions indicated in the upper-right corner of Fig. 1(a). The shifts of the Al 2s and Cr 2p bands have been indicated by dashed lines. The band positions for Al_2O_3 and Cr_2O_3 have been indicated by arrows.

can be observed, the Al 2p band strongly overlaps the Cr 3s band; for this reason, we have additionally measured the Al 2s band. Moreover, the Al 2s band also overlaps strongly with the Si bulk plasmon associated with the Si 2p band. To avoid this drawback, the Al 2s/(Al 2p + Cr 3s) ratio has been measured for the whole range of Al (Cr) concentrations (see Fig. 2), in such a way that knowing the Al 2p + Cr 3s intensities, the equivalent Al 2s intensities can be calculated without any peak fitting even in cases where the overlap with the Si plasmon exists. Experimental results have been represented in Fig. 2 by full squares and they were modeled using Eq. (1)

$$\frac{I(Al\ 2s)}{I(Al\ 2p+Cr\ 3s)} = A\{\ 1-\exp(-B\times C_{Al})\} \quad (1)$$

Here C_{Al} stands for the aluminium nominal concentration, and A and B were used as fitting parameters. The best fitting parameters occurring for $A = 1.1$ and $B = 0.046$.

As observed in Fig. 1, the Al 2s binding energies for the compounds are always below that of Al_2O_3, the Cr 2p binding energy for the compounds is also above that of Cr_2O_3 and the O 1s BE for the compounds is somewhere between those of Cr_2O_3 and Al_2O_3 therefore indicating that Cr–O bonds are more ionic and Al–O bonds are more covalent than in pure Cr_2O_3 and Al_2O_3 oxides. According to T.L. Barr [15], this behavior can be interpreted as due to the formation of a Cr–O–Al mixed oxide instead of the formation of single oxide phases [14,15].

To obtain the atomic concentrations of the different species for the samples CrAl9010, CrAl7510, CrAl2575 and CrAl1090, XPS has been used after Ar^+ bombardment at 3 keV at normal incidence once the surface impurities were removed. Fig. 3 shows (a) the O, Al and Cr concentrations as a function of the Cr (Al) nominal concentrations in the target for samples grown under a constant oxygen flux of 1.25 sccm, and (b) the O, Al and Cr concentrations as a function of the oxygen flux for two different samples (CrAl9010 and CrAl1090). As can be observed, in both cases, the oxygen concentration remains constant at around 60%. Moreover, Fig. 3(a) shows a linear dependence of Al and Cr concentration as a function of the nominal composition of Cr in the target. The linear fit (dashed line) shows that the Al concentration decreases from 40% to 0% as the Cr concentration in the target increases and vice versa. This indicates again the formation of a mixed substitutional oxide of Me_2O_3 type, being Me = Al + Cr. In addition to that, the results of Fig. 3(b) show that the atomic concentrations are nearly independent of the oxygen flux within the studied range (1.25–12.5 sccm).

Additional information on the composition and structure of the mixed oxide films can be obtained from the CDP obtained using XPS and simultaneous Ar^+ bombardment at 3 keV and normal incidence [16]. Fig. 4 shows (a) the CDP measured for the sample CrAl9010 grown with 12.5 sccm of oxygen as a function of the sputtering time

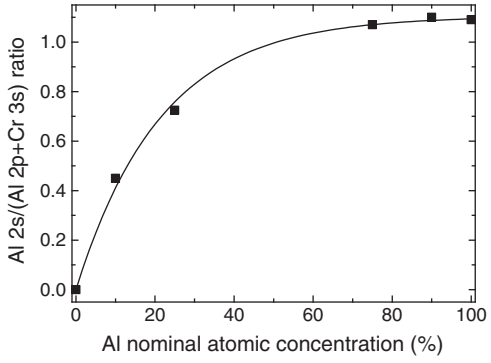

Fig. 2. Evolution of the Al 2s/(Al 2p + Cr 3s) ratio as a function of the Al nominal concentration in the target used for the deposition of the mixed oxide films. The points farthest right and left correspond to Al_2O_3 and Cr_2O_3 standards, respectively.

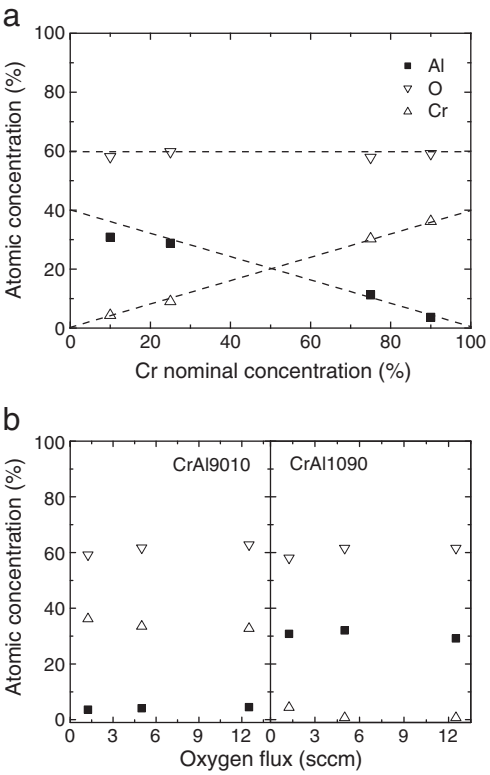

Fig. 3. (a) Oxygen (down triangles), aluminium (full squares) and chromium (up triangles) atomic concentrations as a function of the Cr (Al) target concentration measured using XPS on the Cr–O–Al mixed oxides grown at constant oxygen flux of 1.25 sccm after removal of surface impurities by Ar^+ bombardment. (b) Oxygen, aluminium and chromium atomic concentrations as a function of oxygen flux for two different targets: CrAl9010 and CrAl1090.

using the full O 1s, Cr 2p, Si 2p, C 1s and the corrected Al 2p bands without peak fitting. It should be indicated that the concentration scale has been calibrated using relative sensitivity factors provided by the manufacturer [17]. This is an accurate approach for quantification purposes since it provides the correct stoichiometry for standards of pure Cr, Al and Si oxides. Although no attempt has been made to calibrate the depth scale, it should be indicated that the thickness of the oxide film, measured using stylus methods, is 33 nm therefore leading to a sputtering rate of 0.5 nm/min. The CDP of Fig. 4(a) displays three zones: for very low sputtering times there is the initial surface where the composition is dominated by impurities like C and some segregated Si; for intermediate sputtering times (5 min<t<66 min), it is observed the steady state characterized by a very clean mixed oxide of which the atomic composition is ~61% O, ~34% Cr, ~4% Al and <1% for impurities as C and Si, that is in very good agreement with the expected theoretical values; finally, above 66 min, the CDP is characterized by a strong decrease of the O, Cr and Al compositions and by an increase of the Si amount, representing the interface and the substrate, respectively. It is interesting to notice the apparent increase of the Cr concentration in the interface, displaying a relative maximum, which can be attributed to the presence of metallic Cr species in the interface as can be observed in Fig. 4(b) where the CDP for Cr (Cr_{total}) has been plotted as a function of sputtering time. In addition to that, the results of the peak fitting of the Cr 2p band into two components associated with metallic Cr (Cr_{metal}) and oxidizes species (Cr_{oxide}) have been also plotted.

Fig. 5 shows (a) the peak shape for Cr 2p, (b) for Si 2p, (c) for Al 2p and (d) for the O 1s bands measured at different points of the CDP as indicated in Fig. 4(a): point 1 (film), point 2 (interface) and point 3 (substrate). The Cr 2p band displays contributions at 574.0, 576.1

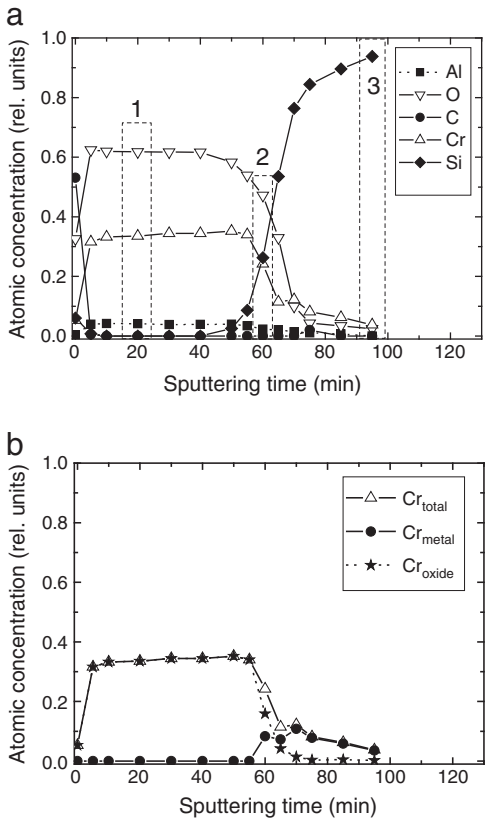

Fig. 4. (a) Concentration depth profile for the Cr–O–Al mixed oxide thin film obtained using target CrAl9010. (b) Idem for the Cr species obtained after peak fitting of the whole Cr 2p band using two components, Cr_{metal} and Cr_{oxide}.

and 578.4 eV that can be attributed to different oxidation states for chromium, that is, metallic chromium (Cr^0), Cr^{3+}, and Cr^{6+}, respectively. The Si 2p band displays contributions at 99.3 eV and 103 eV that should be attributed to pure silicon and silicon oxide, respectively, and the O 1s band shows also two contributions at 530.7 and 532 eV that should be attributed to chromium oxide and either to Si or Al oxides [18], respectively. It is worth to note that, at the interface (2), the Cr 2p band displays a strong metallic contribution and the Si 2p band displays a strong oxide contribution. The severe overlap between the Al 2p and Cr 3s bands does not allow extracting accurate chemical information from spectra of Fig. 5c; however, since the metallic Al 2p band peaks at 72.6 eV, results of Fig. 5c point to the oxide character of such band. The silicon oxide should be attributed to the natural oxide on the surface before Cr–O–Al mixed oxide deposition and the presence of metallic Cr could be explained from thermodynamic considerations. According to the formation enthalpy of Cr_2O_3 (−1134.7 kJ/mol) and Al_2O_3 (−1675.7 kJ/mol) [19], the formation of Al_2O_3 should occur prior to that of Cr_2O_3 in such a way that during the first stages of mixed oxide deposition Cr atoms arriving to the substrate will remain in a metallic state leading to a very thin interfacial film mainly composed of silicon oxide, aluminium oxide and metallic chromium.

It is well known that most binary oxides display oxygen preferential sputtering under Ar^+ bombardment [20]. As a consequence of this phenomenon an altered layer of different composition than that of the original oxidized substrate is established on the surface, its thickness being roughly equal to the ion range and its composition constituted by lower oxidation states of the metals. It is important to note that there are some exceptions as for Al_2O_3, and some disagreement to this rule [20,21]. In general, the published experimental results show that the amount of oxygen depletion increases with the cation mass and is in agreement with predictions put forward by the linear collision cascade theory of sputtering [20]. Since the effective attenuation lengths of Cr 2p, Al 2p, Si 2p and O 1s photoelectron are similar to the thickness of the altered layer for 3 keV Ar^+ bombardment, such a type of surface modification can be easily detected using ARXPS.

Therefore, ARXPS measurements have been carried out on bombarded surfaces in order to elucidate whether oxygen is preferentially sputtered during CDP measurements or not. Fig. 6 shows the measured atomic concentrations as a function of the emission angle, on position 1 of the CDP of Fig. 4 corresponding to the steady state

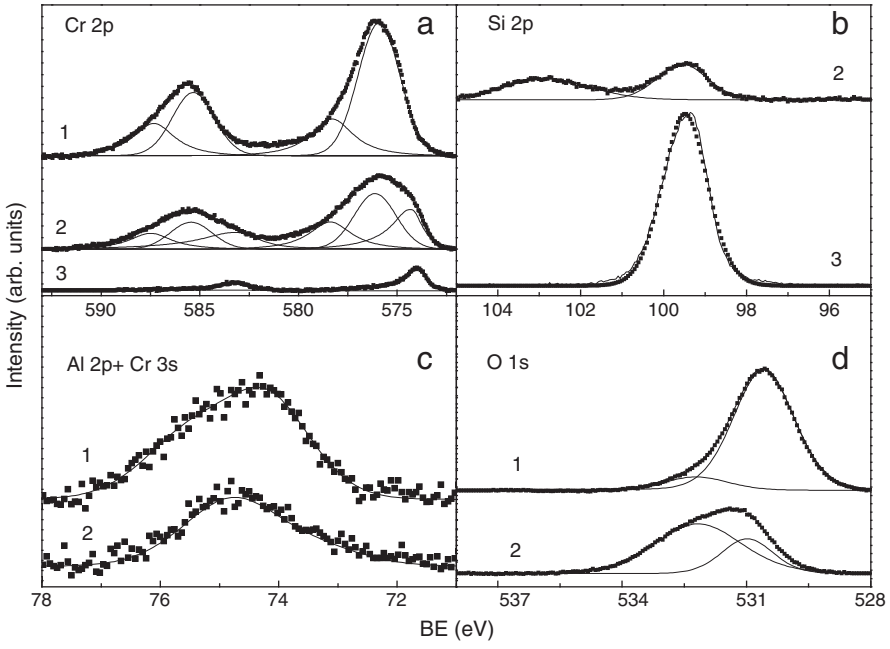

Fig. 5. Peak shapes for (a) Cr 2p, (b) Si 2p, (c) Al 2p + Cr 3s and (d) O (1s) core level spectra measured at different points of the CDP of Fig. 4(a), as indicated in the text.

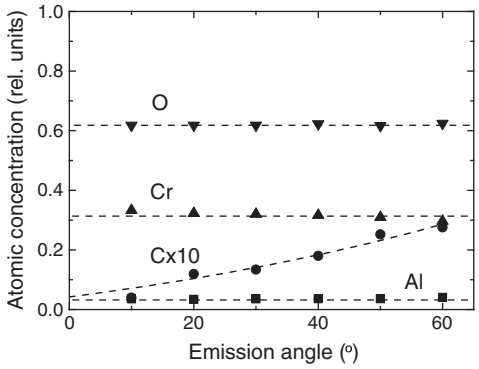

Fig. 6. ARXPS measurements carried out in point (1) of the CDP of Fig. 4(a). The C concentration was multiplied by ten for the sake of clarity.

during Ar^+ bombardment. As observed in Fig. 6, C concentration (multiplied by ten for the sake of clarity) increases with increasing emission angle from 0.6% to 2.7% therefore indicating the presence of a very thin C layer on the instantaneous surface. To calculate concentrations, elemental sensitivity factors provided by the manufacturer [17] and corrected by the transmission function of the operating mode of the analyzer and escape depth effects have been used. It is well known that ARXPS measurements carried out for a film on a substrate display an increase in the film species concentrations with increasing emission angle [21] as in the C case. However, as observed in Fig. 6, ARXPS measurements for the bombarded Cr–O–Al mixed oxide films display a flat profile for Cr, Al and O, their respective concentrations being equal to those of the corresponding stoichimetric film without bombardment, therefore indicating the absence of preferential sputtering effects under Ar^+ bombardment. It is important to indicate that Si traces below 1% atomic concentration (not displayed in Fig. 6) were also detected.

In a first approach, the optical and electrical properties of the mixed oxides are expected to vary between those corresponding to Cr_2O_3 and Al_2O_3 as has been shown for Cr–O–Si [13] and Zr–O–Si [22] mixed oxides. With this in mind, the refractive index could be varied, for instance, by controlling the composition of the mixed oxide as shown above. This is a key point to obtain materials with refractive indexes impossible to obtain for pure oxides. Ellipsometry measurements in the visible range allowed us to determine both the refractive index n and the extinction coefficients k of the films. The oxide layers were fitted using a Cauchy model, which describes the dispersion of the refractive index of the film as a slowly-varying function of wavelength (with an exponential absorption tail [23]). The values of n and k were calculated from the experimental data (psi, ψ and delta, Δ, which describe the polarization state of the light reflected on the surface of the film) using Eqs. (2) and (3).

$$n(\lambda) = A + B/\lambda^2 + C/\lambda^4 \quad (2)$$

$$k(\lambda) = \alpha \cdot \exp\{\beta[12400(1/\lambda - 1/\gamma)]\} \quad (3)$$

Here λ is the wavelength expressed in nm and A, B, C, α (coefficient amplitude), β (exponent factor) and γ (band edge) are fitting parameters. Fig. 7 shows the variation of the refractive index values measured at 600 nm as a function of the Cr concentration in the films for the samples CrAl1090, CrAl2575, CrAl7520 and CrAl9010 grown under a constant oxygen flux of 1.25 sccm. The refractive index of Al_2O_3 and Cr_2O_3 is 1.7 and 2.5, respectively, at 600 nm [10,24], although it is known that they can vary depending on the oxygen content in the film. The refractive index of our oxides lies within the reported values, raising from 1.69 to 2.3 when the amount of chromium in the films increases. This behavior is in accordance with the formation of a mixed substitutional oxide of Me_2O_3 type, being Me = Al + Cr as we mentioned before.

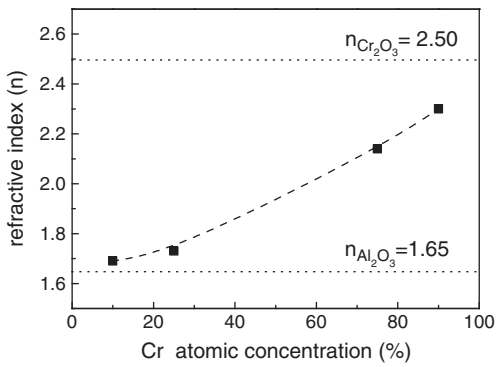

Fig. 7. Refractive index of the Cr–O–Al mixed oxide films measured at 600 nm as a function of the Cr concentration.

4. Conclusions

The synthesis of Cr–O–Al thin film mixed oxides by reactive magnetron sputtering has been investigated. The target compositions were varied from 90% Cr (10% Al) to 10% Cr (90% Al) and the oxygen fluxes in the range 0 to 15 sccm in order to investigate the influence of these parameters on the properties of the films. Ex situ XPS, XPS depth profiles, ARXPS and ellipsometry were used as analytical tools. The main conclusions can be summarized as follows: the chemical information obtained with XPS, as well as the observed chemical shift of the Cr 2p, Al 2s and O 1s bands, points to the formation of mixed substitutional Me_2O_3 oxides (Me = Al + Cr) instead of single oxide phases. Compositions and stoichiometries obtained from CDP using simultaneously XPS and Ar^+ bombardment confirm the formation of such a type of substitutional mixed oxides. The film compositions are related to the target compositions but are roughly independent on the oxygen fluxes (within the analyzed range). The optical properties of the films as the refractive index are controlled through the chemical composition of the film lying between those corresponding to Cr_2O_3 and Al_2O_3. Finally, ARXPS measurements allows ruling out oxygen preferential sputtering during Ar^+ bombardment.

Acknowledgments

The financial support by the Ministerio de Ciencia e Innovación of Spain through the Consolider-Ingenio 2010 programme (CSD2008-00023) and through the project MAT2008-06618-C02 is gratefully acknowledged. REG also wishes to thank the MCINN for the financial support within the Ramón y Cajal Programme.

References

[1] C. Wang, B.Q. Xu, X. Wang, J. Zhao, J. Solid State Chem. 178 (2005) 3500.
[2] A. Kubacka, M. Fernández-García, G. Colón, J. Catal. 254 (2008) 272.
[3] J.C. Anderson, Thin Solid Films 12 (1972) 1.
[4] M. Chigane, M. Izaki, Y. Hatanaka, T. Shinagawa, M. Ishikawa, Thin Solid Films 515 (2006) 2513.
[5] X. Wu, W. Zhang, L. Yan, R. Luo, Thin Solid Films 516 (2008) 3189.
[6] F. Gracia, F. Yubero, J.P. Holgado, J.P. Espinos, A.R. González-Elipe, T. Girardeau, Thin Solid Films 500 (2006) 19.
[7] S. Lisinski, J. Krause, D. Schaniel, L. Ratke, T. Woike, Scr. Mater. 58 (2008) 553.
[8] V.M. Bermudez, W.J. DeSisto, J. Vac. Sci. Technol. A 19 (2) (2001) 576.
[9] E. Sourty, J.L. Sullivan, M.D. Bijker, Tribol. Int. 36 (2003) 389.
[10] P. Hones, M. Diserens, F. Lévy, Surf. Coat. Technol. 120–121 (1999) 277.
[11] M.G. Hutchins, Surf. Technol. 20 (1983) 301.
[12] S. Hong, E. Kim, D.W. Kim, T.H. Sung, K. No, J. Non-Cryst. Solids 221 (1997) 245.
[13] L. Vergara, R. Escobar Galindo, R. Martínez, O. Sánchez, C. Palacio, J.M. Albella, Thin Solid Films 519 (2011) 3509.

[14] M.J. Guittet, J.P. Crocombette, M. Gautier-Soyer, Phys. Rev. B 63 (2001) 125117.
[15] T.L. Barr, J. Vac. Sci. Technol. A9 (1991) 1793.
[16] R. Escobar Galindo, R. Gago, D. Duday, C. Palacio, Anal. Bioanal. Chem. 396 (2010) 2725.
[17] CASA XPS software Ltd., v2.0 User's Manual (2001). www.casaxps.com.
[18] A. Arranz, C. Palacio, J. Phys. Chem. B 106 (2002) 9590.
[19] G.V. Samsonov, The Oxide Handbook, Ifi-Plenum, New York, 1973.
[20] S. Hofmann, J.M. Sanz, J. Trace Microprobe Tech. 1 (1982–83) 213.
[21] C. Palacio, P. Ocón, P. Herrati, D. Díaz, A. Arranz, J. Electroanal. Chem. 545 (2003) 53.
[22] Z. Zhan, H.C. Zeng, J. Non-Cryst. Solids 243 (1999) 26.
[23] H.G. Tompkins, E.A. Irene, Handbook of Ellipsometry, William Andrew Publishing, Norwich, New York, 2005.
[24] P. Frach, U. Heisig, Chr. Gottfried, H. Walde, Surf. Coat. Technol. 59 (1993) 177.